

# **A New Transient Gas Path Diagnostic Method for Gas Turbine Engines with Multi-timescale Inertial Compensation**

**Xiao Cui<sup>1</sup>, Yao Chen<sup>1</sup>, Jinwei Chen<sup>2</sup>, Huisheng Zhang<sup>1</sup>**

<sup>1</sup>The Key Laboratory of Power Machinery and Engineering of Education Ministry, Shanghai Jiao Tong University  
No. 800 Dongchuan Road, Minhang District, Shanghai, PR China  
cuixiao23@sjtu.edu.cn; 15121165293@163.com; chenjinweituihou@sjtu.edu.cn

<sup>2</sup>College of Smart Energy, Shanghai Jiao Tong University  
No. 800 Dongchuan Road, Minhang District, Shanghai, PR China  
zhslm@sjtu.edu.cn

**Abstract** – Gas turbine is an advanced power machine commonly used in aviation, Marine and power generation. The existing steady-state diagnosis model is limited to encompassing merely 20% of the flight process for aero gas turbines. To broaden the scope of data available for fault diagnosis, this study introduces a fault diagnosis, considering the dynamic attributes of the system. On the basis of the traditional steady-state model, the dynamic characteristics of the system are considered, including mechanical inertia, volumetric inertia and thermal inertia. A gas turbine model integrating multi-timescale inertial elements is formulated. Within this framework, mechanical inertia is harnessed to determine shaft speed, volumetric inertia is instrumental in adjusting combustor pressure, and thermal inertia is factored in while computing outlet temperature. These multi-time scale inertial features can be obtained from design handbook and experimental data. A comparative evaluation is conducted between the proposed dynamic method and the conventional steady-state approach. the results demonstrate that the multi-time scale inertial compensation model is capable of encompassing the operational data under dynamic conditions. The proposed model yields the anticipated diagnostic outcomes in both normal and faulty operation scenarios.

**Keywords:** gas turbine, gas path analysis, fault diagnosis, dynamic diagnosis, multi-timescale

## **1. Introduction**

Gas turbine (GT) engine is a kind of internal combustion turbomachinery, which has the advantages of fast start-stop speed, high efficiency and compact structure. It has been widely used in aircraft[1], Marine[2], power generation[3], etc. During the operation of GT, high heat flux, high mechanical stress and thermal stress caused by external air pollutants and internal high-intensity combustion will lead to various failures of the equipment, affecting the reliability of the equipment, operating costs and pollutant emissions. Its main components, including compressor, combustor and turbine, will appear scaling, mechanical damage, corrosion, thermal deformation and other faults, resulting in changes in the geometric parameters of the gas turbine flow channel (surface roughness, flow shape, and flow area). These lead to a decline in the efficiency and flow performance of the gas path components. However, these defects cannot be directly measured. Therefore, it is particularly important to understand the degree of performance degradation of gas turbines.

Numerous studies have delved into fault diagnosis within the realm of GT. Nayeri et al. introduced a fault detection and isolation system based on an ensemble-based hierarchical classifier, aimed at scrutinizing scaling faults, sensor faults and simultaneous faults of different components[4]. Castillo et al. advocated for the adoption of nonlinear data-driven models and inverse problem theory to simplify the diagnostic model of gas turbines[5]. Due to the smearing effect when measuring problems with high noise levels, Ying et al. used an improved particle swarm optimization algorithm to estimate the health state of gas turbines[6]. Zhou et al. proposed a data coordination model that considers relative residuals and correlation of variables[7]. Nonetheless, these studies primarily revolve around diagnosing equipment performance under steady-state conditions. These methods are unable to offer reliable diagnostic results for dynamic conditions, which constitute more than half of the flight operations.

Aiming at the problem of gas turbine under dynamic conditions, several notable research have been pursued. Chen et al. proposed a gas turbine fault diagnosis method based on time series measurement[8]. Their methodology leveraged changes in shaft speed data to gauge the power imbalance existing between the compressor and turbine components. Huang et al. categorized all working conditions into four typical working conditions. A small deviation diagnosis model was established

for typical start-stop state and high dynamic state[9]. Liu et al. proposed a performance prediction framework based on expertise and deep learning techniques[10]. Chen et al. established a real-time fault diagnosis system by combining the gas turbine model with unscented Kalman filter[11]. Zhou et al. designed a gas turbine fault diagnosis and prediction method that combines gas path analysis and long short-term memory to realize the coupling of fault diagnosis and prediction process[12]. Cui et al. used kernel principal component analysis to establish a deep learning fault diagnosis model, and integrated it with extreme learning machine at the decision level to further improve the accuracy of fault diagnosis[13]. Nevertheless, the majority of these strategies tackle dynamic conditions by employing a data-driven methodology that hinges on historical operational data. In the case of aero gas turbines, failure sample data is often scarce.

The steady-state model utilized in the conventional gas path diagnosis method is enhanced in this paper. The mathematical model of GT is improved by considering the multi-timescale inertial, including volume inertia, mechanical inertia and thermal inertia. These parameters can be obtained from the gas turbine's handbook and operating data. The effects of these parameters on fault diagnosis accuracy are contrasted under dynamic conditions. The introduction of these parameters extends the application scope of the diagnostic model to dynamic conditions.

## 2. Methodology

### 2.1. problem description

The research object of this study is a two-shaft aero engine. A schematic of the engine is shown in Fig. 1. The model comprises a fan, two compressors, a combustor, two turbines and a mixer. During operation, air is drawn through the fan and split into two streams: one flows directly through the bypass duct to the outlet, while the other stream enters the compressor. The compressed gas from the compressor enters the combustor, where it is mixed with the fuel and ignited. Subsequently, the high-temperature and high-pressure gas is expelled after performing external work through the turbine.

The fan, low-pressure compressor, and low-pressure turbine are mounted on the same rotating shaft, operating at speed  $N_1$ . Similarly, the high-pressure compressor and high-pressure turbine are coupled on another rotating shaft, running at speed  $N_2$ .

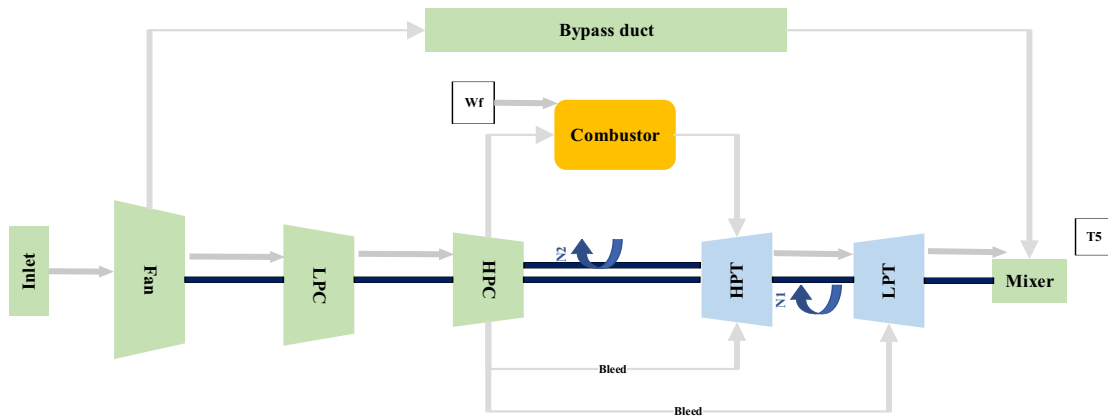


Fig. 1: Schematic diagram of aero gas turbine

The steady-state diagnosis model commonly used in industry can obtain satisfactory results under steady-state conditions. However, the data of full flight are characterized by intense oscillations. Commonly, these transient data would be ignored for the gas path diagnosis. As a result, the GPA only covers about 20% flight process at present. the most part of the flight process would not be diagnosed. Insufficient coverage problems would occur fault diagnosis in the entire flight process when using the steady-state diagnosis model.

## 2.2. Gas path analysis

GPA is a method of obtaining gas path health status from measurable parameters[14]. The flow diagram of the gas path fault diagnosis method is shown in Fig. 2. The gas path fault diagnosis method includes three parts: measurement parameters, simulation model, and solving algorithm. The GPA process is the reverse of the simulation process of the physical model. The inputs of the GPA model are boundary conditions  $x$  and measurement data  $y$ , and its output is fault feature  $D$ . The whole solving process of GPA model is an iterative process. In the  $i$ -th iterative process, the iterative process  $D^i$  and boundary condition  $x$  are inputted into the gas turbine physical model  $f()$  to obtain the simulation data  $\hat{y}$  of the measurement parameters. The iterative process ends when the simulation data  $\hat{y}$  and actual measurement data  $y$  satisfy the tolerance condition.

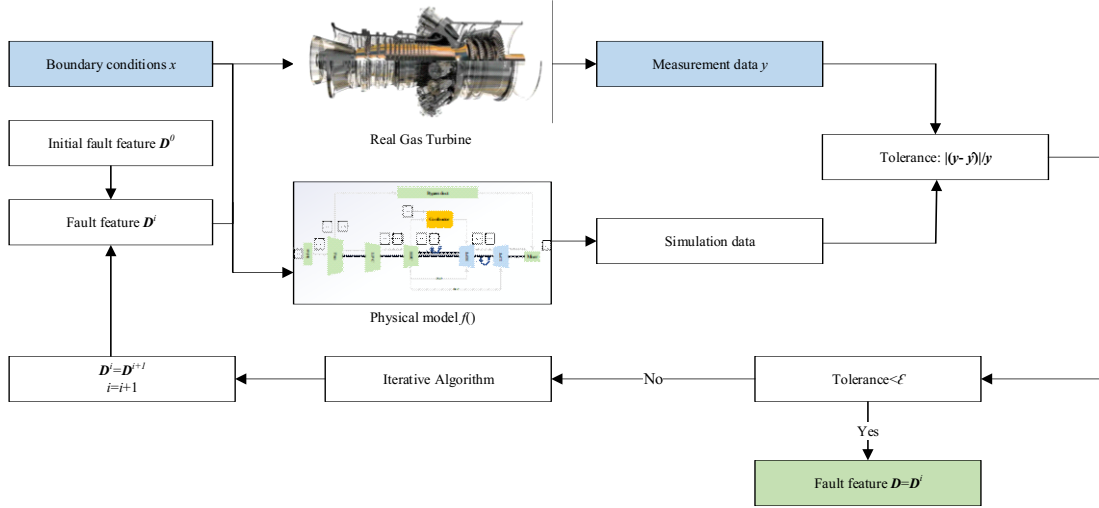


Fig. 2: Process of gas path diagnosis model

## 2.3. Dynamic Model

The traditional steady-state model cannot give sufficiently accurate results under dynamic conditions. To broaden the applicability of the current model, it is necessary to consider the dynamic response characteristics of the equipment. This section describes a method to improve the dynamic performance of the model by considering the multi-timescale inertias of the gas turbine. The mechanical and volume inertias are obtained based on the design handbook. The thermal inertia is identified by the operation data.

When the volume inertia of the combustor is considered, the difference in the inlet and outlet flow of the combustor will cause the pressure change

$$\frac{dp_3}{dt} = \frac{R_g T_3}{V} (G_{HC} + G_{fuel} - G_{HT}) \quad (1)$$

Where,  $R_g$  is gas constant,  $V$  is the volume of combustor, which can be obtained from the design handbook.

The rate of change of speed is given by equation (2)-(3) when the power consumption of compressor and fan is not equal to the output power of turbine:

$$\frac{dN_1}{dt} = \frac{900}{I_1 \pi^2 N_1} (P_{LT} - P_{LC} - P_{Fan}) \quad (2)$$

$$\frac{dN_2}{dt} = \frac{900}{I_2 \pi^2 N_2} (P_{HT} - P_{HC}) \quad (3)$$

Where,  $I_1$  and  $I_2$  is the moment of inertia of the rotating shaft.

The outlet temperature should satisfy equation (4) when thermal inertia is considered

$$\frac{dT_5}{dt} = \frac{k_f}{\rho C_p} (T_5 - T_5) \quad (4)$$

Where,  $k_f$  is the coefficient of thermal inertia, which is derived from the measurement data.  $\rho$  is the density, and  $C_p$  is the specific heat capacity of the discharged gas.

### 3. Discussion of results

The experiment is conducted on the ground test bench of a newly manufactured aero engine in a healthy state. An acceleration experiment is performed, and the selected data range of speed change is shown in Fig. 3. Data in the range of 400 to 480 seconds were selected to analysis the diagnostic accuracy. Here the relative speed is increased from 94.2% to 98.9% and remain stable.

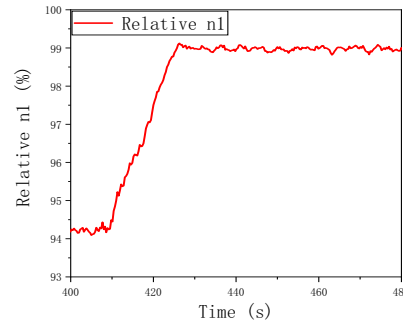


Fig. 3: The relative speed n1 within the chosen range of experimental data

The exhaust gas temperature results obtained by simulation are shown in the Fig. 4. The initial relative exhaust temperature is 0.982. The temperature starts to rise gradually at around 408s and reaches stability at around 460 seconds. The stable temperature is about 0.997. By observing the curve trend in the figure, the simulation results of the proposed model are consistent with the real data, seeing the orange line. The maximum error occurs at 425 seconds, with an error of 0.183%. As a comparison, the results of steady-state model and those without thermal inertia are given. The results show that the results of the model which unconsidered heat inertia has a similar trend to the steady-state model. Although the temperature of the two models also began to rise at around 408s, due to insufficient inertial factors considered, the result reached a stable temperature at around 430 seconds. This time is same with the moment when the speed is stable in the input data. This means the simulation results of the model will be significantly different from the real situation during and after the speed change. The results in Fig. 4 confirm this view. When the time is 417s, the results show the maximum error. The maximum error of the steady-state model is 0.686%. That of the dynamic model without thermal inertia is 0.628%, which is slightly smaller than that of the steady-state model. This is also in line with expectations.

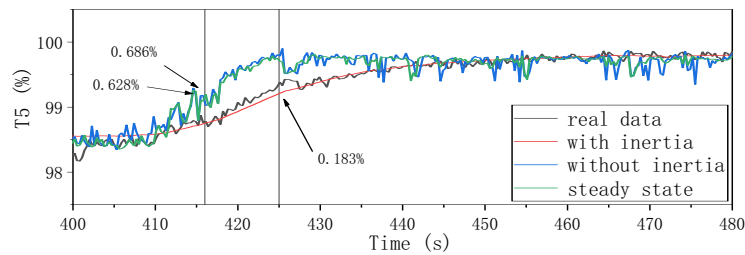


Fig. 4: the exhaust gas temperature of different models

The results for fan and low-pressure compressor (LPC) are given in Fig. 5. The maximum diagnostic errors results are shown in Table 1. For the fault diagnosis results of fans, the results of the two models have obvious differences. The flow rate and efficiency degradation of the output of the dynamic diagnosis model are always near 0, which is consistent with experimental conditions. However, the output of the steady-state diagnosis model gradually moves away from 0 at about 408s, reaches the maximum value at about 422 seconds, and then gradually recovers. This result results in a large error in the calculation of the gas condition parameters passing the bypass duct, affecting the exhaust temperature results shown in Fig. 4. As for the flow degradation of LPC, seeing Fig. 5(c), there is little difference between the results of the two models, and the maximum error obtained by the dynamic model is slightly smaller than that of the steady-state model. However, as for the efficiency degradation of low-pressure compressor, seeing Fig. 5(d), the maximum error of 1.51% obtained by the dynamic model is significantly smaller than that of 2.07% obtained by the steady-state model. In short, the dynamic diagnosis model effectively reduces the error in the transient process.

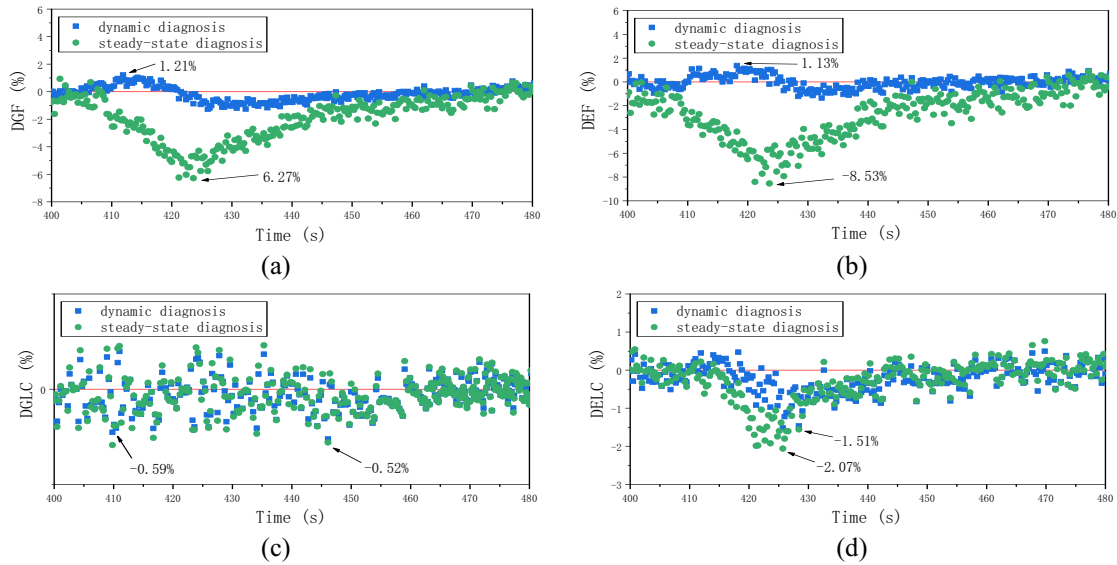


Fig. 5: Fault diagnosis results when the GT is healthy. (a) the flow degradation of fan; (b) the efficiency degradation of fan; (c) the flow degradation of LPC; (d) the efficiency degradation of LPC.

Table 1: Comparison of the maximum diagnostic errors in health status data

	DGF	DEF	DGLC	DELC
Steady-state diagnosis	-6.27%	-8.53%	-0.59%	-2.07%
Dynamic diagnosis	1.21%	1.13%	-0.52%	-1.51%
Reduction in error	80.70%	86.75%	11.86%	27.05%

Subsequently, a fan scaling fault was injected into the experimental data, with DGF=3.5% and DEF=1%. The results of the diagnosis are shown in Fig. 6, and the maximum diagnostic errors results are displayed in Table 2. As can be seen from the Fig. 6, the diagnosis result of the proposed model is always near the expected value, while the diagnosis result of the steady-state diagnosis model shows a tendency to deviate from the expected value under dynamic conditions. Among them, the biggest error appears in the efficiency degradation results of the low-pressure turbine (LPT). The maximum error of the dynamic model is 1.55%, and that of the steady-state model is 3.06%. Such error is likely to cause the model to give wrong diagnosis results or false alarms under dynamic conditions, resulting in safety hazards or waste of maintenance funds.

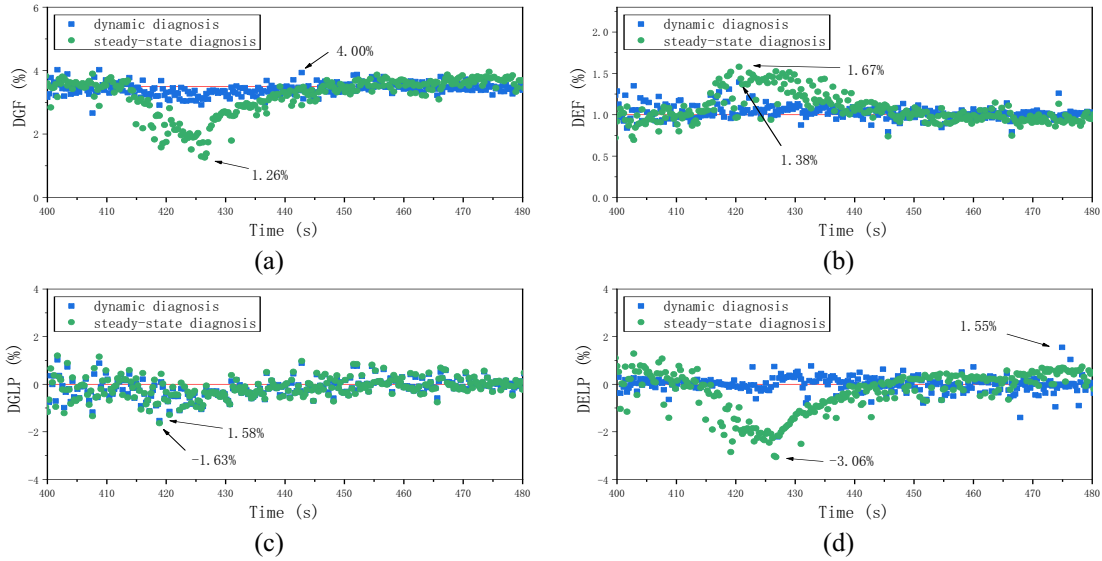


Fig. 6: Fault diagnosis results when a fan scaling fault is injected. (a) the flow degradation of fan; (b) the efficiency degradation of fan; (c) the flow degradation of LPT; (d) the efficiency degradation of LPT.

Table 2: Comparison of the maximum diagnostic errors in a fan scaling fault data

	DGF	DEF	DGLP	DELP
Steady-state diagnosis	-2.24%	0.67%	-1.63%	-3.06%
Dynamic diagnosis	0.50%	0.38%	-1.58%	1.55%
Reduction in error	77.68%	43.28%	3.07%	49.35%

## 4. Conclusion

In this paper, a dynamic diagnosis method with multi-timescale inertias is proposed. The main work and conclusions are as follows:

- **A dynamic diagnosis model with multi-time scale inertia is established.** A dynamic diagnosis model of gas turbine is established considering mechanical inertia, volumetric inertia and thermal inertia. The introduced multi-time scale inertia can be obtained according to the design handbook and experimental data.
- **Better simulation of transient characteristics.** The simulation performance of the model is analysed using the data of the acceleration process. The error of the proposed model is smaller than the steady-state model. The maximum diagnostic error of the proposed model is DGF=1.21%, which is reduced by 80.70% compared with the steady-state model.
- **Higher diagnostic accuracy.** The error of the diagnosis model is compared in the case of injection fault. The results of the dynamic model always agree with the expected values. However, the steady-state model deviates from the expected value in the dynamic range. The maximum error of the dynamic model is DGLP=1.58%, whereas that of the steady-state model is 1.63%. In the context of the discussed fault data, the error is reduced by up to 77.68% compared to the traditional model.

In conclusion, the proposed model extends the range of diagnosable data from steady-state conditions to dynamic conditions and has been effectively verified in both health data and fault data.

## References

- [1] Z. Wei, S. Zhang, S. Jafari, and T. Nikolaidis, "Gas turbine aero-engines real time on-board modelling: A review, research challenges, and exploring the future," *Progress in Aerospace Sciences*, vol. 121, p. 100693, 2020.

- [2] U. Campora, C. Cravero, and R. Zacccone, "Marine gas turbine monitoring and diagnostics by simulation and pattern recognition," *International Journal of Naval Architecture and Ocean Engineering*, vol. 10, no. 5, pp. 617-628, 2018.
- [3] J. Li and Y. Ying, "A Novel Machine Learning Based Fault Diagnosis Method for All Gas-Path Components of Heavy Duty Gas Turbines With the Aid of Thermodynamic Model," *IEEE Transactions on Reliability*, vol. 73, no. 4, pp. 1805-1818, 2024.
- [4] M. R. Nayeri, B. Nadjari Araabi, and B. Moshiri, "Fault detection and isolation of gas turbine: Hierarchical classification and confidence rate computation," *Journal of the Franklin Institute*, vol. 359, no. 17, pp. 10120-10144, 2022.
- [5] I. G. Castillo, I. Loboda, and J. L. Pérez Ruiz, "Data-Driven Models for Gas Turbine Online Diagnosis," *Machines*, vol. 9, no. 12, p. 372, 2021.
- [6] Y. Ying, Y. Cao, S. Li, and J. Li, "Nonlinear Steady-State Model Based Gas Turbine Health Status Estimation Approach with Improved Particle Swarm Optimization Algorithm," *Mathematical Problems in Engineering*, vol. 2015, no. 1, p. 940757, 2015.
- [7] D. Zhou, D. Huang, L. Zhang, J. Hao, and S. Ma, "A global thermodynamic measurement data reconciliation model considering boundary conditions and parameter correlations and its applications to natural gas compressors," *Measurement*, vol. 172, p. 108972, 2021.
- [8] Y.-Z. Chen, E. Tsoutsanis, C. Wang, and L.-F. Gou, "A time-series turbofan engine successive fault diagnosis under both steady-state and dynamic conditions," *Energy*, vol. 263, p. 125848, 2023.
- [9] D. Huang, S. Ma, D. Zhou, X. Jia, Z. Peng, and Y. Ma, "Gas path fault diagnosis for gas turbine engines with fully operating regions using mode identification and model matching," *Measurement Science and Technology*, vol. 34, no. 1, p. 015903, 2023.
- [10] Z. Liu, M. Hou, G. Sa, Y. Wang, X. Xin, and J. Tan, "Gas turbine multi-working conditions identification and performance prediction based on deep learning and knowledge," *Energy*, vol. 308, p. 133011, 2024.
- [11] X. Cheng, H. Zheng, Q. Yang, P. Zheng, and W. Dong, "Surrogate model-based real-time gas path fault diagnosis for gas turbines under transient conditions," *Energy*, vol. 278, p. 127944, 2023.
- [12] H. Zhou, Y. Ying, J. Li, and Y. Jin, "Long-short term memory and gas path analysis based gas turbine fault diagnosis and prognosis," *Advances in Mechanical Engineering*, vol. 13, no. 8, p. 16878140211037767, 2021.
- [13] C. Du, R. Zhong, Y. Zhuo, X. Zhang, F. Yu, F. Li, Y. Rong and Y. Gong, "Research on fault diagnosis of automobile engines based on the deep learning 1D-CNN method," *Engineering Research Express*, vol. 4, no. 1, p. 015003, 2022.
- [14] U. L. A, *Gas turbine engine parameter interrelationships*. USA: Hamilton Standard Division of United Aircraft Corporation, 1969.